

## Circulating ANGPTL2 Levels Increase in Humans and Mice Exhibiting Cardiac Dysfunction

Zhe Tian, MD, PhD; Keishi Miyata, MD, PhD; Jun Morinaga, MD, PhD; Haruki Horiguchi, PhD; Tsuyoshi Kadomatsu, PhD; Motoyoshi Endo, MD, PhD; Jiabin Zhao, MD; Shunshun Zhu, BSc; Taichi Sugizaki, MD, PhD; Michio Sato, MD; Kazutoyo Terada, PhD; Takahiro Okumura, MD, PhD; Toyoaki Murohara, MD, PhD; Yuichi Oike, MD, PhD

**Background:** Recently, it was reported that angiotensin-like protein 2 (ANGPTL2) secreted from a pathologically stressed heart accelerates cardiac dysfunction in an autocrine/paracrine manner, and that suppression of ANGPTL2 production in the heart restored cardiac function and myocardial energy metabolism, thereby blocking heart failure (HF) development. Interestingly, circulating ANGPTL2 concentrations reportedly increase in HF patients, suggesting a possible endocrine effect on cardiac dysfunction. However, it remains unclear why circulating ANGPTL2 increases in those subjects and whether circulating ANGPTL2 alters cardiac function in an endocrine manner.

**Methods and Results:** It was found that circulating ANGPTL2 levels are positively correlated with left atrial diameter and pulmonary capillary wedge pressure, and are inversely proportional to the percent of ejection fraction in patients with dilated cardiomyopathy. Furthermore, in mice, circulating ANGPTL2 concentrations increased as HF developed following transverse aorta constriction (TAC), and were inversely correlated with the percent of fractional shortening. Interestingly, although circulating ANGPTL2 concentrations significantly increased in transgenic mice overexpressing keratinocyte-derived ANGPTL2, no pathological cardiac remodeling was seen. Furthermore, it was observed that there was no difference in HF development between transgenic mice and controls following TAC surgery.

**Conclusions:** Circulating ANGPTL2 levels increase in subjects experiencing cardiac dysfunction. However, circulating ANGPTL2 does not promote cardiac dysfunction in an endocrine manner, and increased levels of circulating ANGPTL2 seen during HF are a secondary effect of increased ANGPTL2 secretion from stressed hearts in HF pathologies.

**Key Words:** ANGPTL2; DCM; Heart failure; Mouse TAC model

Heart failure (HF) is a leading cause of mortality in the developed world, with a 5-year mortality rate of approximately 50%, a rate equal to that of many cancers.<sup>1,2</sup> Recently, the number of HF patients has rapidly increased to an estimated 26 million people worldwide, an outcome now recognized as a HF pandemic.<sup>3,4</sup> HF prevalence increases among older people due to cumulative effects of cardiovascular risk factors over a lifetime,<sup>5</sup> and HF represents a major public health problem in developed countries. Notably, Japan has the highest proportion of older people in the world: 26.3% of the population were aged 65 years or older in 2015 (www.worldbank.org). Accordingly, a HF pandemic in Japan is predicted by

2030.<sup>6,7</sup> Therefore, clarification of molecular mechanisms underlying HF development is necessary to develop effective therapeutic strategies to combat this outcome.

Angiotensin-like protein 2 (ANGPTL2), a member of the ANGPTL family,<sup>8</sup> is a secreted glycoprotein that contributes to tissue homeostasis by enhancing tissue remodeling in an autocrine/paracrine manner.<sup>9–11</sup> However, excessive ANGPTL2 signaling promotes chronic inflammation and subsequent irreversible pathological tissue remodeling, resulting in various lifestyle- or aging-associated diseases, such as obesity, metabolic syndrome, type 2 diabetes, atherosclerotic vascular disease, and some cancers.<sup>11–19</sup> Several studies report that ANGPTL2 is expressed

Received March 26, 2017; revised manuscript received August 17, 2017; accepted August 21, 2017; released online September 8, 2017  
Time for primary review: 37 days

Department of Molecular Genetics, Graduate School of Medical Sciences (Z.T., K.M., J.M., H.H., T.K., M.E., J.Z., S.Z., T.S., M.S., K.T., Y.O.), Department of Immunology, Allergy, and Vascular Biology, Graduate School of Medical Sciences (K.M.), Institute of Resource Developmental and Analysis (H.H.), Kumamoto University, Kumamoto; Department of Cardiology, Nagoya University Graduate School of Medicine, Nagoya (T.O., T.M.), Japan

The Guest Editor for this article was Dr. Yoshihiko Saito.

The first two authors contributed equally to this work (Z.T., K.M.).

Mailing address: Yuichi Oike, MD, PhD, Department of Molecular Genetics, Graduate School of Medical Sciences, Kumamoto University, 1-1-1 Honjo, Chuo-ku, Kumamoto 860-8556, Japan. E-mail: oike@gpo.kumamoto-u.ac.jp

ISSN-1346-9843 All rights are reserved to the Japanese Circulation Society. For permissions, please e-mail: cj@j-circ.or.jp

**Table 1. Clinical Characteristics of Patients With Dilated Cardiomyopathy**

| Variable                                     | n (%) or median (IQR); range      |
|--|-----------------------------------|
| n  | 63                                |
| Age  | 58 (44–64); 30–75                 |
| Sex (M/F)                                    | 42/21                             |
| NYHA (I/II/III)                              | 26/31/6                           |
| BNP (pg/mL)                                  | 89.75 (52.25–281.25); 3.9–1,515.9 |
| <b>Ultrasonic echocardiographic analysis</b> |                                   |
| EF (%)                                       | 30 (24–40); 13–55                 |
| LVDd (mm)                                    | 62 (56–66); 46–88                 |
| LVDs (mm)                                    | 51 (45–56); 35–83                 |
| LAD (mm)                                     | 40 (35–46); 23–62                 |
| E/A  | 2.58 (1.74–3.39); 0.70–5.36       |
| LVMI (g/m <sup>2</sup> )                     | 156 (121–199); 94–409             |
| <b>Cardiac catheterization analysis</b>      |                                   |
| HR (beats/min)                               | 77 (69–90); 52–117                |
| CO (L/min)                                   | 4.45 (3.70–5.325); 1.90–7.70      |
| CI (L/min/m <sup>2</sup> )                   | 2.6 (2.2–3.1); 1.2–4.3            |
| sBP (mmHg)                                   | 120.5 (105.75–137); 79–182        |
| dBp (mmHg)                                   | 74.5 (64.75–87); 50–107           |
| PCWP (mmHg)                                  | 11 (7–14); –2 to 28               |
| sPA (mmHg)                                   | 25 (19–32); 11–61                 |
| dPA (mmHg)                                   | 10 (7–14); –1 to 30               |
| RA (mmHg)                                    | 6 (3–8); –2 to 13                 |

Values are presented as mean  $\pm$  SEM or number (n) and percentage (%) for categorical variables. BNP, brain natriuretic peptide; CI, cardiac index; CO, cardiac output; dBp, diastolic blood pressure; DCM, dilated cardiomyopathy; dPA, diastolic pulmonary artery pressure; E/A, ratio of peak early mitral inflow velocity to peak late diastolic mitral inflow velocity during atrial contraction; EF, ejection fraction; HR, heart rate; LAD, left atrial dimension; LVDd, left ventricular end-diastolic dimension; LVDs, left ventricular end-systolic dimension; LVMI, left ventricular mass index; NYHA, New York Heart Association; PCWP, pulmonary capillary wedge pressure; RA, mean atrial pressure; sBP, systolic blood pressure; sPA, systolic pulmonary artery pressure.

in the heart,<sup>8,11,12</sup> although its cardiac function is unclear. Recently, we reported that ANGPTL2 secreted from pathologically stressed heart accelerates cardiac dysfunction, and that suppression of ANGPTL2 production from the heart restored cardiac function and myocardial energy metabolism, thereby blocking HF development.<sup>11,20</sup> In that study, although we observed increased levels of circulating ANGPTL2 in mice with cardiac dysfunction, we did not address whether ANGPTL2 affects cardiomyocytes in an endocrine or autocrine/paracrine manner. Interestingly, another study reported that circulating ANGPTL2 levels are higher in HF patients than in controls, and that cardiac function is inversely correlated with levels of ANGPTL2 circulating in the periphery,<sup>21</sup> although this study did not address underlying mechanisms. These findings indicate, overall, that circulating ANGPTL2 levels increase and are associated with cardiac dysfunction under HF conditions, although whether circulating ANGPTL2 promotes pathological cardiac remodeling in this manner is unknown.

Here, we report that heart tissue itself is a critical source of increased circulating ANGPTL2 levels under HF conditions. We also found that circulating ANGPTL2 concentrations are positively correlated with cardiac dysfunction. To assess whether increased ANGPTL2 in circulation altered heart function, we performed pathological and physiological analysis of transgenic (Tg) mice overexpressing ANGPTL2 in keratinocytes (*K14-Angptl2* Tg mice), as circulating ANGPTL2 concentrations significantly increase in these mice. Interestingly, we found that increased

ANGPTL2 in circulation itself did not promote cardiac dysfunction in these mice, suggesting that increased levels of circulating ANGPTL2 seen under HF conditions are a secondary effect of increased ANGPTL2 secretion from a stressed heart in HF pathologies.

## Methods

### Human Studies

Sixty-three consecutive patients with dilated cardiomyopathy (DCM) (42 men and 21 women; mean age  $\pm$  SEM, 54.8  $\pm$  12.5 years; **Table 1**) were enrolled in the study. Twenty-six were classified as New York Heart Association (NYHA) class I, 31 as class II, and 6 as class III. Individuals with an episode of acute HF within the previous 3 months or with renal dysfunction (estimated glomerular filtration rate [eGFR] of <30 mL/min/1.73 m<sup>2</sup>) were excluded from the study. All subjects underwent coronary angiography to exclude coronary artery disease, as well as an endomyocardial biopsy to exclude myocarditis or specific muscle disease. DCM was defined as the presence of both a left ventricular (LV) ejection fraction (EF) of <50% (as revealed by contrast left ventriculography) and a dilated LV cavity in the absence of coronary artery stenosis of >50%, valvular heart disease, arterial hypertension, and secondary cardiac muscle disease attributable to any known systemic condition.<sup>22</sup> No patient had a history of acute viral myocarditis or familial DCM. There was also no evidence that immune triggers influenced DCM

development in any patient. Patients were in a stable condition before referral to Nagoya University Hospital for cardiac catheterization. Written informed consent was obtained from each patient before cardiac catheterization, and the study was approved by the Human Ethics Committee of the Nagoya University School of Medicine, Japan (protocol approval No. 359-7; March 16, 2015).

### Cardiac Catheterization Analysis

All patients underwent diagnostic right and left heart catheterization, as described previously.<sup>23</sup> In brief, pulmonary arterial wedge pressure (PCWP) and cardiac output (CO) were measured using a Swan-Ganz catheter inserted through the right internal jugular vein. Cardiac index (CI) was calculated as follows: CI=CO per body surface area (L/min/m<sup>2</sup>). Central aortic systolic and diastolic blood pressure were measured using a 6F fluid-filled pigtail catheter inserted through the right radial or femoral artery. Serum ANGPTL2 levels were determined using human ANGPTL2 ELISA kits (IBL, Fujioka, Japan).

### Ultrasonic Echocardiographic (UCG) Analysis of Human Patients

Two-dimensional UCG analysis was performed using a ViVid 7 system (ViVid 7; GE Healthcare, Milwaukee, WI, USA), as described previously.<sup>23</sup> Analysis included measurement of LV end-diastolic dimension (LVDd), LV end-systolic dimension (LVDs), and left arterial dimension (LAD). Percentage of EF (%EF) was calculated from LVDd and LVDs. LV mass index (LVMI) was calculated from two-dimensional measurements based on a formula approved by the American Society of Echocardiology.<sup>24</sup>

### Animal Studies

All experimental procedures were approved by the Kumamoto University Ethics Review Committee for Animal Experimentation. Mice were fed a normal diet (ND; CE-2; CLEA, Tokyo, Japan), bred in a mouse house with automatically controlled lighting (12h on, 12h off), and maintained at a stable temperature of 23°C. Genetically engineered mice used in the study were: *Angptl2* conditional knockout mice (*Angptl2<sup>Flox/Flox</sup>*) on a C57BL/6N background,<sup>20</sup> transgenic (Tg) mice overexpressing *Cre* driven by the murine  $\alpha$ MHC promoter ( $\alpha$ MHC-*Cre*) on a C57BL/6N background,<sup>25</sup> and Tg mice overexpressing *Angptl2* in keratinocytes (*K14-Angptl2*) on an FVB/N background.<sup>16,26</sup> The *db/db*, *KK-Ay*, and *KK* mice were purchased from CLEA Japan.

### Establishment of Hypertrophy Mouse Models

Male mice approximately 10 weeks old (body weight of 23–25 g) were subjected to pressure overload using transverse aorta constriction (TAC) surgery, as described previously.<sup>20</sup> Echocardiography analysis was performed after TAC surgery, as described previously.<sup>20</sup>

### Histological Analysis

Histological analysis was performed, as described previously.<sup>20</sup> In brief, mouse heart tissue sections were stained with hematoxylin and eosin (H&E; Wako, Osaka, Japan) to evaluate morphology or Masson's Trichrome (Muto Pure Chemicals, Tokyo, Japan) to evaluate cardiac fibrosis. The fibrotic area was calculated, using Image J software (National Institutes of Health), as the summation of blue-stained areas divided by total ventricular area. Slides were

mounted and examined using a BIOREVO BZ-9000 microscope (Keyence, Osaka, Japan).

### Real-Time Quantitative Reverse-Transcription-Polymerase Chain Reaction (RT-PCR) Analysis

Real-time quantitative RT-PCR analysis was performed, as described previously.<sup>20</sup> Relative transcript abundance was normalized to that of *18S* rRNA levels in mouse and human samples. Primer sets used for RT-PCR are listed in Table S1.

### Western Blot Analysis

Western blot analysis was performed, as described previously.<sup>20</sup> In brief, total protein (20  $\mu$ g) or serum (0.1  $\mu$ l) proteins were separated by sodium dodecyl sulfate-polyacrylamide gel electrophoresis (SDS-PAGE) and transferred to poly vinylidene fluoride (PVDF) membranes. Membranes were incubated with anti-AKT (#9272S), anti-p-AKT (s473) (#9271), anti-p-AKT (T308) (#4056; Cell Signaling Technology, Danvers, MA, USA), or anti-Serca2a (ab3625; Abcam, Cambridge, MA) antibodies diluted 1:1,000 at 4°C overnight. After washing with phosphate-buffered saline with 0.1% Tween 20 (PBST), membranes were incubated with 1:2,000 diluted horseradish peroxidase (HRP)-conjugated sheep anti-rabbit IgG (GE Healthcare Life Science, Piscataway, NJ, USA) antibodies at room temperature for 60 min. For *Angptl2* immunoblotting, membranes were incubated with biotinylated goat anti-*Angptl2* antibody (BAF1444; R&D Systems, Minneapolis, MN, USA) diluted 1:3,000 at 4°C overnight. After washing with PBST, membranes were incubated with HRP-conjugated streptavidin (Thermo Fisher Scientific Inc., Waltham, MA, USA) diluted 1:6,000 at room temperature for 60 min. Internal controls were mouse anti-Hsc70 (sc-7298; Santa Cruz Biotechnology, Santa Cruz, CA, USA) and diluted HRP-conjugated sheep anti-mouse IgG (GE Healthcare Life Science) antibodies (both diluted 1:2,000), which served as primary and secondary antibodies, respectively. Hsc70 was used for normalization.

### Recombinant Adeno-Associated Virus (AAV) Treatment

Recombinant AAV treatment was performed, as described previously.<sup>20</sup> In brief, production and purification of recombinant AAV6 vectors were conducted at Takara Bio Inc. In brief, for shRNA synthesis, single-stranded DNA oligos harboring mouse *Angptl2*-targeting siRNA and complementary strands were designed as follows: top 5'-CTAGAGCCAGAAAGCGAGTACTATATAGTGCTCCTGGTTGTATAGTACTCGCTTTCTGGCTTTTTTA-3' and bottom 5'-CTAGTAAAAAGCCAGAAAGCGAGTACTATACAAACCAGGAGCACTATAGTACTCGCTTCTGGCT-3'; Scramble-top 5'-CTAGAGTCTTAATCGCGTATAAGGCTAGTGCTCCTGGTTGGCCTTATACGCGATTAAGACTTTTTA-3' and Scramble-bottom 5'-CTAGTAAAAAGTCTTAATCGCGTATAAGGCCAACCAGGAGCACTAGCCTTATACGCGATTAAGACT-3'. Single-stranded oligos (sh*Angptl2* and shScramble) were annealed and cloned into the pAAV-2xU6 vector (Takara Bio Inc). For analysis of TAC animals, 10-week-old male C57BL/6Njcl mice (CLEA Japan) were subjected to TAC surgery and 2 weeks later anesthetized with 2% isoflurane and intravenously injected with recombinant AAV6 vectors at 3 $\times$ 10<sup>10</sup> vg.

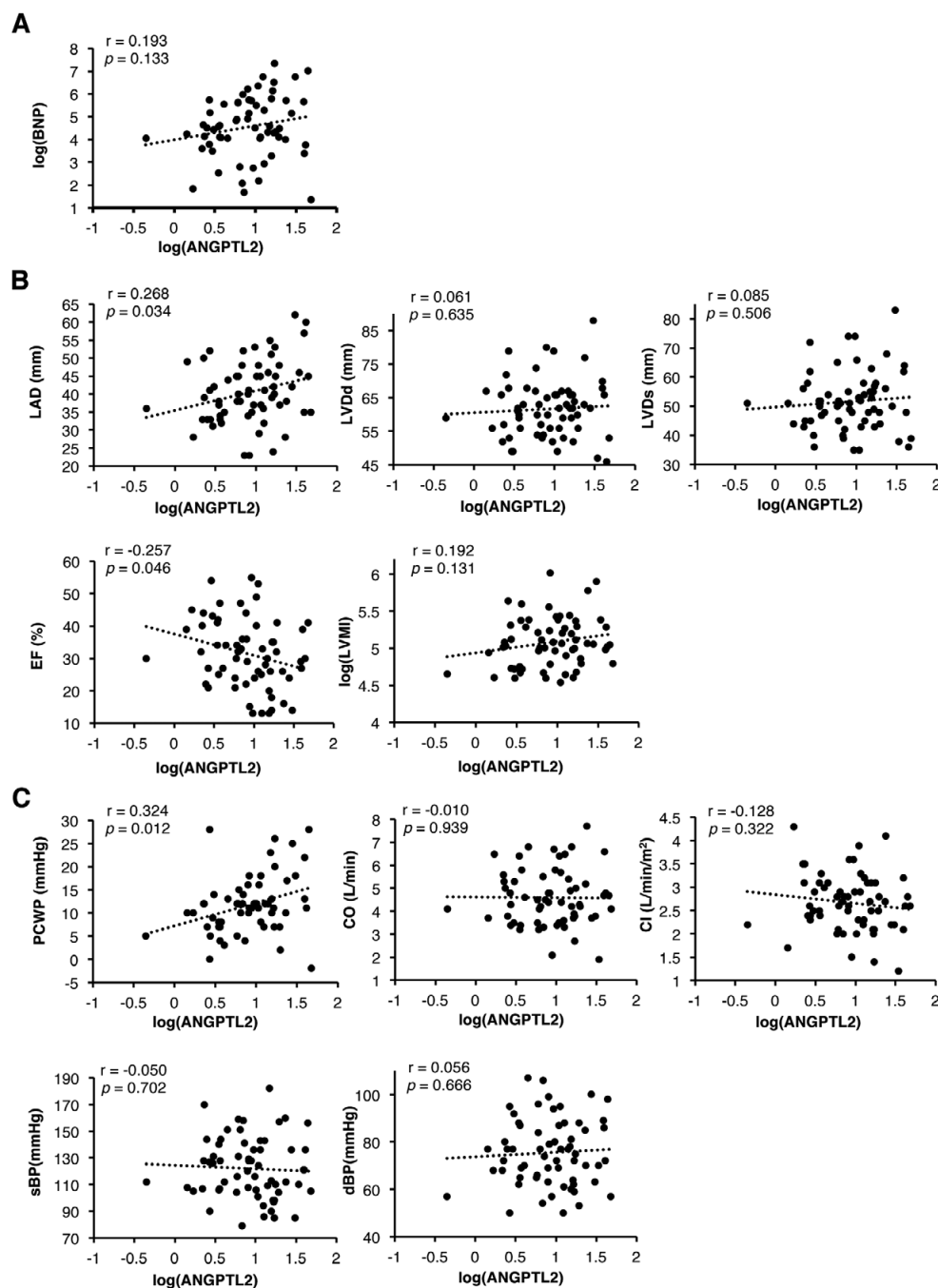


**Figure 1.** Relationship of circulating angiopoietin-like protein 2 (ANGPTL2) levels to heart failure (HF)-associated clinical parameters. Scatter plots show correlation between circulating ANGPTL2 levels and brain natriuretic peptide (BNP) (**A**), echocardiographically derived parameters (left atrial diameter (LAD), left ventricular end-diastolic dimension (LVDd), left ventricular end-systolic dimension (LVDs), percent of ejection fraction (EF), and left ventricular mass index (LVMI)) (**B**); right heart catheterization analysis-derived parameters (pulmonary capillary wedge pressure (PCWP), CO (cardiac output), and CI (cardiac index)) (**C, Upper rows**), and left heart catheterization analysis-derived parameters (systolic blood pressure (sBP), diastolic blood pressure (dBP); and **C, Bottom rows**). Also shown is Pearson's correlation coefficient for rho.

### Statistical Analysis

In human studies, Pearson's test and correlation coefficients were used to evaluate relationships between serum ANGPTL2 levels and clinical variables (e.g., BNP, ultra-

sonic echocardiographically derived parameters, and hemodynamic measurement). For multiple linear regression analyses, a generalized linear model was used. Statistical analyses were performed using JMP Pro 12 software (SAS

Institute, Cary, NC, USA). In animal studies, no statistical methods were used to determine sample size, but sample sizes were similar to those used in previous reports.<sup>20,27</sup> No exclusion/inclusion criteria were applied to mice used in this study. Group allocation and outcome assessment were performed in a blinded manner. In vitro experiments were repeated at least three times. All values were reported as mean  $\pm$  SEM. Data were assessed with 2-group comparisons of variables using an unpaired 2-tailed t-test, with multiple

**Table 2. Generalized Linear Regression Analysis (Adjusted for Age and Sex)**

| Parameters | $\beta$ (95% CI)        | P value |
|------------|-------------------------|---------|
| LAD        | 5.830 (0.921, 10.740)   | 0.0207  |
| EF         | -5.685 (-12.225, 0.855) | 0.0872  |
| PCWP       | 3.912 (0.183, 7.640)    | 0.0401  |

Abbreviations as in Table 1.

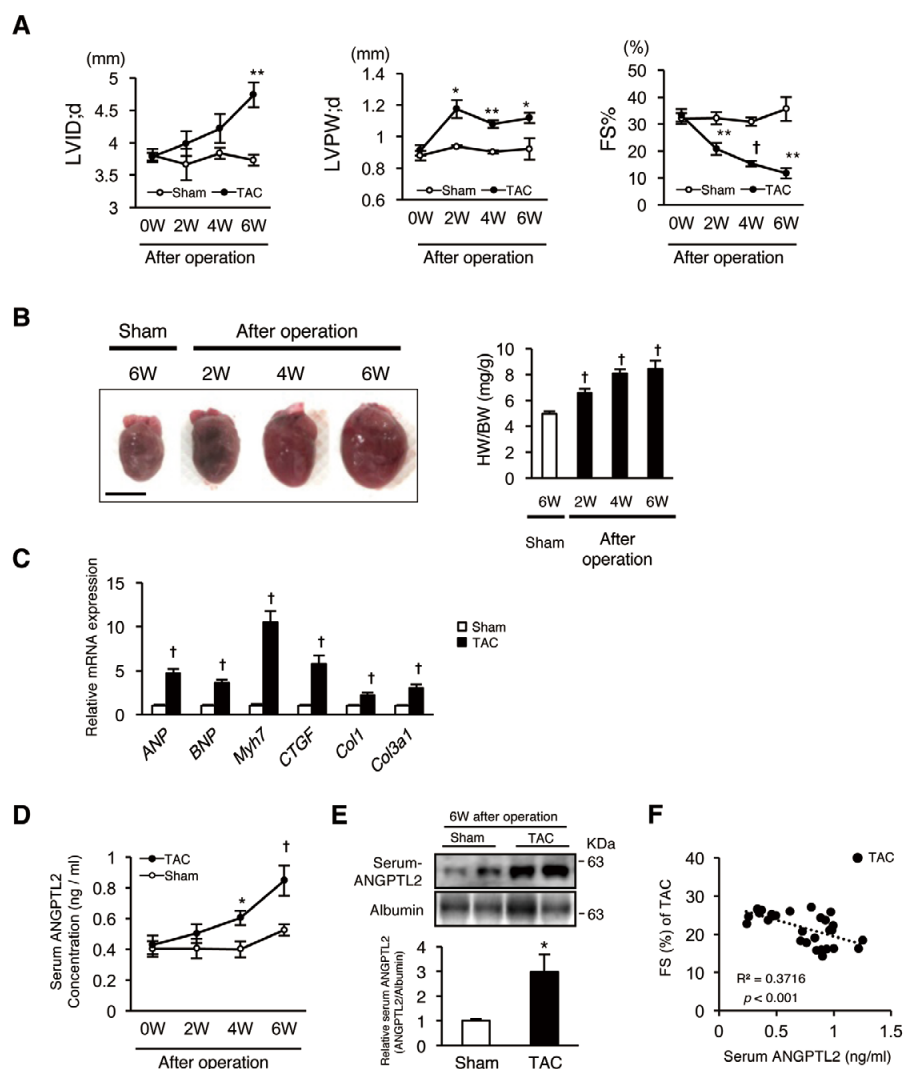


**Figure 2.** Circulating ANGPTL2 levels increase in mice following transverse aorta constriction (TAC) surgery. **(A)** Echocardiographically left ventricular end-diastolic internal diameter (LVID;d; **Left**), diastolic left ventricular posterior wall thickness (LVPW;d; **Middle**), and percent fractional shortening (FS%; **Right**) before surgery (0W) and 2, 4, and 6 weeks after surgery in sham and TAC-operated wild-type (WT) mice (n=8–10 per group). **(B)** Representative images of a heart 6 weeks after sham surgery and 2, 4, and 6 weeks after post-TAC surgery (**Left**). Calculation of heart weight/body weight (HW/BW) ratio (**Right**) at 2, 4, and 6 weeks after sham or TAC surgery (n=8–10 per group). Scale bar: 5 mm. **(C)** Relative expression of mRNAs associated with HF and cardiac fibrosis. Sham-operated control values were set to 1 (n=8–10 per group). **(D)** Enzyme-linked immunosorbent assay (ELISA) for circulating ANGPTL2 protein before surgery and at 2, 4, and 6 weeks after surgery in sham and TAC-operated WT mice (n=8–10 per group). **(E)** Representative western blots and quantitation of serum ANGPTL2 protein from WT mice 6 weeks after TAC or sham surgery (n=13 per group). Albumin served as the loading control. Sham-operated control values were set to 1. **(F)** Scatter plots showing the correlation between serum ANGPTL2 protein and %FS from WT mice at 2, 4, and 6 weeks after TAC (n=8–10 per group) Data are presented as mean  $\pm$  SEM. Statistical significance was determined by using a Student's t-test. \*P<0.05, \*\*P<0.01, †P<0.001 between groups. Abbreviations as in Figure 1.

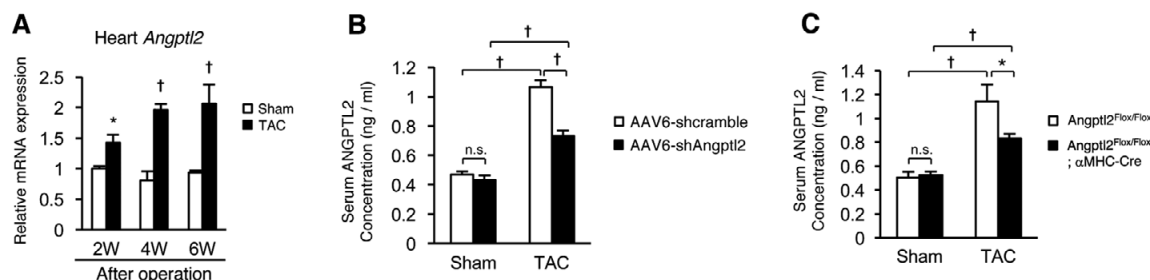


**Figure 3.** Cardiomyocyte-secreted ANGPTL2 contributes to increases in circulating ANGPTL2 levels after TAC surgery. **(A)** Expression levels of *Angptl2* mRNA in heart 2, 4, and 6 weeks after sham or TAC surgery (n=6–9 per group). Values of mRNA expression levels in sham-operated control mice after surgery were set to 1. **(B)** Serum ANGPTL2 protein concentration 6 weeks after TAC surgery in sham- or TAC-operated mice injected with of AAV6-shScramble or AAV6-shAngptl2 ( $3 \times 10^{10}$  vg/mouse) 2 weeks after surgery (n=6–10 per group). **(C)** Serum ANGPTL2 protein concentration in *Angptl2*<sup>Flx/Flx</sup> and *Angptl2*<sup>Flx/Flx</sup>; αMHC-Cre mice 6 weeks after TAC or sham surgery (n=5 per group). Data are presented as mean ± SEM. Statistical significance was determined by using a Student's t-test **(A)** or one-way ANOVA **(B,C)**. \*P<0.05, †P<0.001 between groups. Abbreviations as in Figures 1,2.

comparisons by 1- or 2-way ANOVA with Tukey's multiple comparisons test between each group. A value of P<0.05 was considered statistically significant.

## Results

### Circulating ANGPTL2 Levels Correlate With LAD and PCWP in Patients With DCM

To determine whether circulating ANGPTL2 levels were correlated with cardiac function, we assessed brain natriuretic peptide (BNP) levels and undertook UCG analysis and hemodynamic measurement in DCM patients (**Figure 1A–C**). The study population consisted of 63 patients with DCM, and their characteristics are shown in **Table 1**. Interestingly, LAD and PCWP were positively correlated with circulating ANGPTL2 levels ( $r=0.268$ ,  $P=0.034$  and  $r=0.324$ ,  $P=0.012$ , respectively), while %EF was inversely correlated with those levels ( $r=-0.257$ ,  $P=0.046$ ) in DCM patients. The statistically significant positive correlation between circulating ANGPTL2 concentrations and LAD and PCWP remained unchanged after adjustment for age and sex ( $P=0.0207$ ,  $P=0.0401$ , respectively; **Table 2**). Taken together, we found that circulating ANGPTL2 levels are positively correlated with cardiac dysfunction in patients with DCM.

### Circulating ANGPTL2 Levels Increase in Mice Following TAC Surgery

To assess whether circulating ANGPTL2 levels change in a HF mouse model, we measured those levels in the blood of mice showing cardiac dysfunction induced by TAC surgery-dependent pressure overload. After TAC surgery, we evaluated pathological cardiac remodeling by analyzing UCG (LV dimension in end-diastolic phase (LVDd)) and thickness of the LV posterior wall (LVPW), percent of fractional shortening of LV (% of FS), heart weight/body weight (HW/BW) ratio, and expression of markers of HF (*ANP*, *BNP*, and *Myh7*) and cardiac fibrosis (*CTGF*, *Coll*, and *Col3a1*) (**Figure 2A–C**). Enzyme-linked immunosorbent assay (ELISA) of mouse sera revealed gradually increasing circulating ANGPTL2 concentrations after TAC surgery (**Figure 2D**). Six weeks after TAC, western blotting also

revealed that circulating ANGPTL2 concentrations were significantly increased compared to sham-operated controls (**Figure 2E**). Circulating ANGPTL2 levels were also inversely correlated with %FS in the TAC model ( $r^2=0.3716$ ,  $P<0.001$ , **Figure 2F**). These results indicate overall that in mice, circulating ANGPTL2 levels are positively correlated with cardiac dysfunction.

### Increased Circulating ANGPTL2 Following TAC Surgery Is Derived From Cardiomyocytes

We next asked which tissues contribute to increased circulating ANGPTL2 levels after TAC surgery in mice. Expression of *Angptl2* mRNA in the heart was significantly increased compared to that of sham-operated controls throughout a 2-, 4- and 6-week period of TAC-induced HF development (**Figure 3A**). We then asked whether lowering ANGPTL2 expression in the heart would decrease circulating ANGPTL2 concentrations after TAC surgery by employing systemic delivery of recombinant adeno-associated virus serotype 6 (AAV6) vectors, which preferentially transduce cardiac muscle.<sup>20</sup> We then compared circulating ANGPTL2 protein levels after TAC surgery between mice delivered *Angptl2* shRNA cassettes to the heart by intravenous injection of a recombinant AAV6 vector harboring *Angptl2* shRNA ( $3 \times 10^{10}$  vg/mouse) and controls similarly injected with scramble control shRNA ( $3 \times 10^{10}$  vg/mouse). ANGPTL2 protein levels in the hearts of mice receiving scramble control shRNA after TAC surgery were higher than those seen in sham-operated mice, and those increases were blocked in mice receiving *Angptl2* shRNA (data not shown), as previously reported.<sup>20</sup> Relevant to circulating ANGPTL2, levels seen in scramble control shRNA in TAC-operated mice increased remarkably compared with those in sham-operated mice, whereas increases were significantly attenuated in TAC-operated mice injected with *Angptl2* shRNA (**Figure 3B**). Moreover, we compared circulating ANGPTL2 levels after TAC between cardiomyocyte-specific *Angptl2* conditional knockout mice (*Angptl2*<sup>Flx/Flx</sup>; αMHC-Cre) and (*Angptl2*<sup>Flx/Flx</sup>) controls. ANGPTL2 protein levels in the hearts of control mice increased compared with levels in sham-operated mice, and those increases were attenuated in

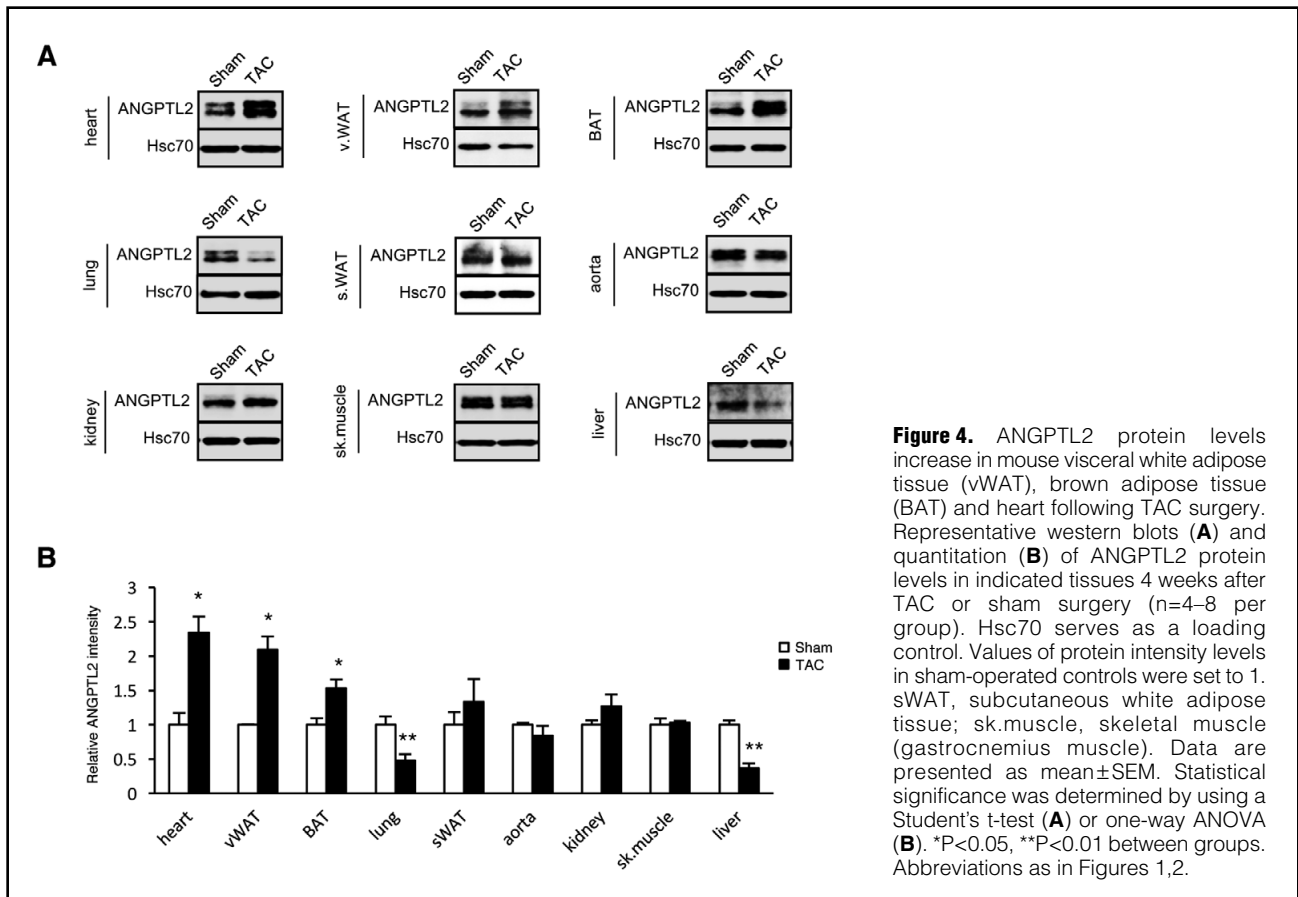


**Figure 4.** ANGPTL2 protein levels increase in mouse visceral white adipose tissue (vWAT), brown adipose tissue (BAT) and heart following TAC surgery. Representative western blots (**A**) and quantitation (**B**) of ANGPTL2 protein levels in indicated tissues 4 weeks after TAC or sham surgery (n=4–8 per group). Hsc70 serves as a loading control. Values of protein intensity levels in sham-operated controls were set to 1. sWAT, subcutaneous white adipose tissue; sk.muscle, skeletal muscle (gastrocnemius muscle). Data are presented as mean±SEM. Statistical significance was determined by using a Student's t-test (**A**) or one-way ANOVA (**B**). \*P<0.05, \*\*P<0.01 between groups. Abbreviations as in Figures 1,2.

*Angptl2<sup>Flox/Flox</sup>;αMHC-Cre* mice (data not shown). Circulating ANGPTL2 levels were remarkably higher in TAC-operated compared with sham-operated *Angptl2<sup>Flox/Flox</sup>* control mice, while those increases were significantly attenuated in TAC-operated *Angptl2<sup>Flox/Flox</sup>;αMHC-Cre* mice (**Figure 3C**). We conclude that heart, and cardiomyocytes in particular, are the primary sources of increased ANGPTL2 protein circulating in mice following TAC-induced cardiac dysfunction.

#### ANGPTL2 Protein Levels Increase in Mouse Visceral White Adipose Tissue (vWAT) and Brown Adipose Tissue (BAT) Following TAC Surgery

Increases in circulating ANGPTL2 levels are not completely blocked after cardiomyocyte-specific ANGPTL2 knockdown (**Figure 3B**), suggesting that other tissues produce ANGPTL2 in these mice. To test this possibility, we compared ANGPTL2 protein levels in various tissues of TAC- and sham-operated mice. Four weeks after surgery, ANGPTL2 protein levels significantly increased in vWAT and BAT, as well as in the hearts of TAC-relative to sham-operated controls (**Figure 4A,B**), suggesting that mice adipose tissue is an additional source of circulating ANGPTL2 levels following TAC-induced cardiac dysfunction.

#### Increased Circulating ANGPTL2 Protein Does Not Promote Pathological Hypertrophy or Cardiac Dysfunction

We next asked whether increased circulating ANGPTL2 has an endocrine effect on cardiac dysfunction. As reported previously,<sup>16,26</sup> we confirmed that circulating ANGPTL2

protein levels increased approximately 3-fold in transgenic mice overexpressing ANGPTL2 in the skin under the control of the *K14* promoter (*K14-Angptl2 Tg* mice) compared to those seen in wild-type controls (**Figure 5A**). In contrast, cardiac ANGPTL2 protein levels were comparable in both groups (**Figure 5B**). Interestingly, the increased ANGPTL2 levels in circulation were comparable to those in wild-type mice with HF pathologies.

We recently reported that ANGPTL2 secreted from cardiomyocytes perturbs cardiac function by inactivating the AKT-SERCA2a  $Ca^{2+}$  handling cascade in transgenic mice overexpressing ANGPTL2 in cardiomyocytes under control of the *αMHC* promoter (*αMHC-Angptl2 Tg* mice).<sup>20</sup> Therefore, we questioned whether circulating ANGPTL2 has an endocrine effect on that activity. Western blotting analysis revealed that the AKT-SERCA2a  $Ca^{2+}$  handling cascade was not inactivated in *K14-Angptl2 Tg* mice (**Figure 5C**). Furthermore, analysis of UCG and HW/BW, as well as histology and RT-PCR, revealed no differences in cardiac phenotypes or marker expression between *K14-Angptl2 Tg* and wild-type controls with or without TAC (**Figure 5D–H**), suggesting that increased ANGPTL2 levels in circulation itself does not have effect on cardiac remodeling in HF pathologies.

Given that adipose tissues also contribute to increased circulating ANGPTL2 levels (**Figure 4**), we questioned whether adipose tissue-derived ANGPTL2 protein promoted cardiac dysfunction. We previously reported that diet-induced obese mice showed increased ANGPTL2 expression in adipose tissue and increased levels of



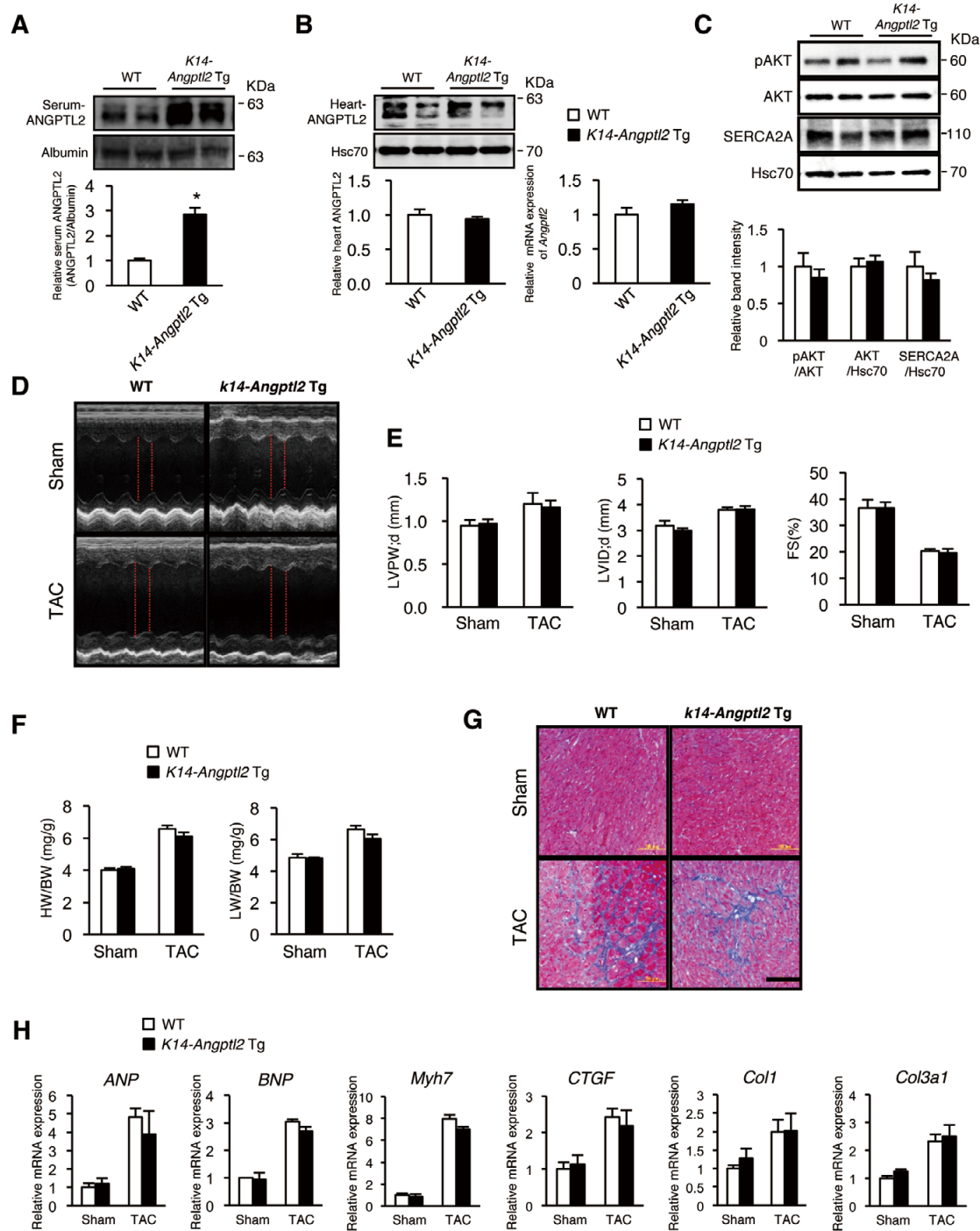


**Figure 5.** Circulating ANGPTL2 protein has no effect on cardiac function or development of cardiac hypertrophy in *K14-ANGPTL2 Tg* mice. (A) Representative western blots and quantification of serum ANGPTL2 protein levels in *K14-Angptl2 Tg* or WT littermate mice (n=5–6 per group). Albumin serves as a control. WT values were set to 1. (B) Representative western blots and quantification of ANGPTL2 protein and ANGPTL2 mRNA levels in hearts of *K14-Angptl2 Tg* and WT mice. Hsc70 serves as a control. WT values were set to 1 (n=6 per group). (C) Representative immunoblot and quantitation of p-AKT, AKT and SERCA2A protein levels in hearts of *K14-Angptl2 Tg* and WT mice (n=6 per group). Hsc70 serves as a control. Values from WT were set to 1. (D) Shown are representative M-mode echocardiography recordings from *K14-Angptl2 Tg* and WT littermate mice 4 weeks after sham surgery (Upper row) or TAC (Bottom row) surgery. (E) Echocardiographic quantitation of LVPW;d (Left), LVID;d (Middle), and fractional shortening (FS; Right). (F) Heart weight/body weight (HW/BW) ratio (Left) and lung weight/body weight (LW/BW) ratio (Right) of *K14-Angptl2 Tg* or WT littermate mice. (G) Sections of Masson's Trichrome-stained heart tissue from *K14-Angptl2 Tg* or WT littermate mice 4 weeks after sham (Upper row) or TAC (Bottom row) surgery. Scale bar: 100  $\mu$ m. (H) Relative expression of mRNAs associated with HF and cardiac fibrosis (n=6 per group). WT values were set to 1. Data are presented as mean  $\pm$  SEM. Statistical significance was determined by using a Student's t-test. \*P<0.05 between genotypes. Abbreviations as in Figures 1,2.



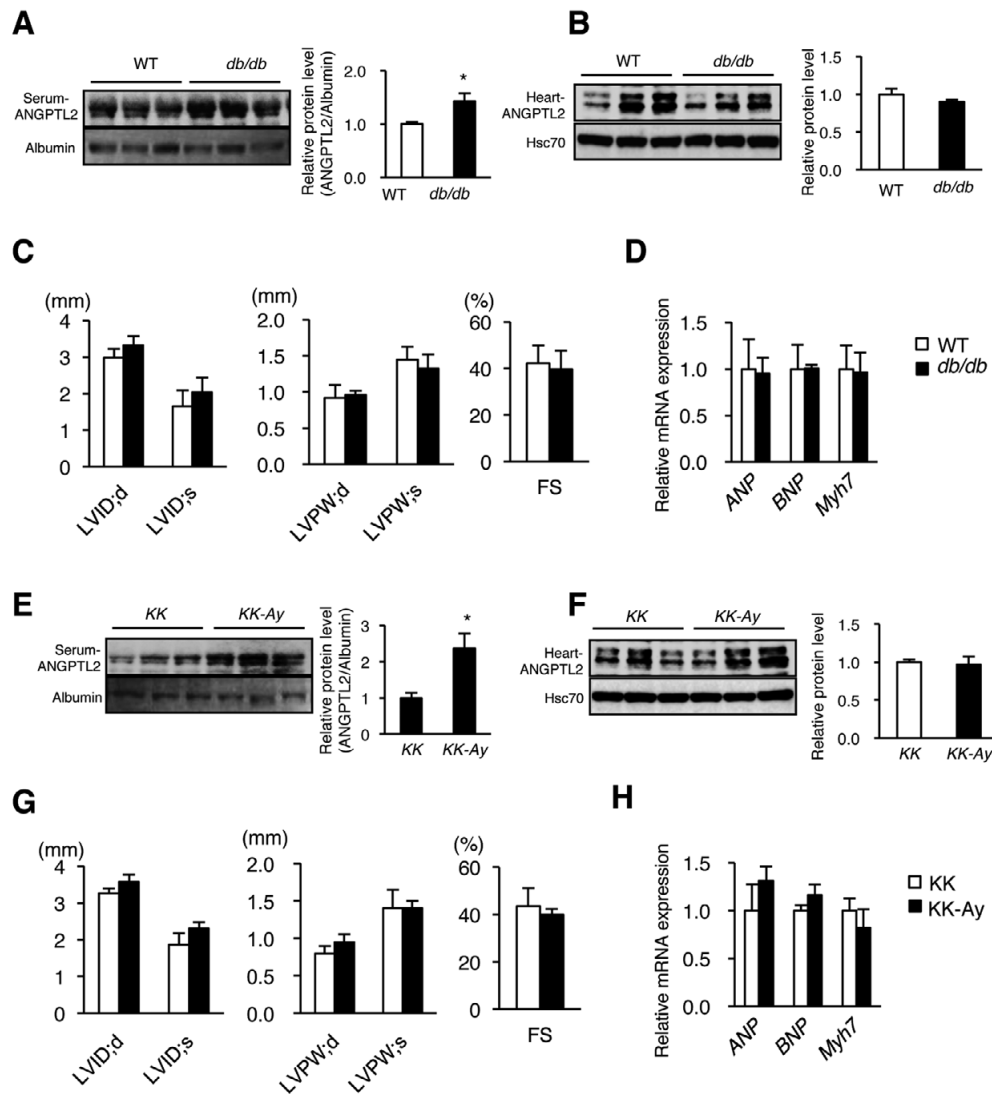


**Figure 6.** Adipose tissue-derived ANGPTL2 protein does not alter cardiac function. Representative western blots and quantification of ANGPTL2 protein levels in serum (**A**) and heart (**B**) of 12-week-old *db/db* or WT littermate mice ( $n=7$  per group). Albumin or Hsc70 served as a control. ANGPTL2 protein levels in WT mice were set to 1. Echocardiographic quantitation of left ventricular end-diastolic internal diameter (LVID; **Left**), left ventricular posterior wall thickness (LVPW; **Middle**), and %FS (**Right**; **C**) and relative expression of mRNAs associated with HF (**D**) in the hearts of 12-week-old *db/db* or WT littermate mice ( $n=3$  per group). WT mRNA expression levels were set to 1. Representative western blots and quantification of ANGPTL2 protein levels in serum (**E**) and hearts (**F**) of 12-week-old *KK-Ay* or *KK* littermate mice ( $n=7$  per group). Albumin or Hsc70 served as a control. ANGPTL2 protein levels in *KK* mice were set to 1. Echocardiographic quantitation of LVID (**Left**), LVPW (**Middle**), and %FS (**Right**; **G**) and relative expression of mRNAs associated with HF (**H**) in the hearts of 12-week-old *KK-Ay* or *KK* littermate mice ( $n=3$  per group). mRNA levels in *KK* mice were set to 1. Data are presented as mean $\pm$ SEM. Statistical significance was determined by using a Student's *t*-test. \* $P<0.05$  between genotypes. Abbreviations as in Figures 1,2.

circulating ANGPTL2 protein.<sup>12</sup> Here, using 2 models of genetically obese diabetic mice (*db/db* and *KK-Ay*), we observed elevated ANGPTL2 protein levels in circulation compared with controls (**Figure 6A,E**), whereas ANGPTL2 protein levels in heart tissues of both models were comparable to controls (**Figure 6B,F**). UCG analysis revealed no cardiac hypertrophy, ventricular dilatation, or cardiac dysfunction in *db/db* or *KK-Ay* mice compared with non-obese controls (**Figure 6C,G**). Moreover, in both models, *ANP*, *BNP*, and *Myh7* expression in the heart was unchanged relative to the controls (**Figure 6D,H**). We con-

clude that increased ANGPTL2 protein derived from adipose tissue does not promote cardiac dysfunction, which also suggests no endocrine effects of ANGPTL2 in circulation on cardiac function.

## Discussion

This study demonstrates that circulating ANGPTL2 levels positively correlate with cardiac dysfunction in DCM patients and in a TAC-induced mouse HF model. Our study also demonstrates that, in mice, increased ANGPTL2 lev-

els are primarily due to secretion by cardiomyocytes in conditions of TAC-induced cardiac dysfunction, although adipose tissues also contribute to these effects. Our findings indicate that increased ANGPTL2 in circulation likely does not cause or accelerate pathological hypertrophy or cardiac dysfunction in mice, but is rather a result of increased secretion from stressed heart in HF pathologies.

Recently, Huang et al reported that circulating ANGPTL2 levels in HF patients were higher than those in control individuals, and that cardiac function was inversely correlated with levels of ANGPTL2 circulating in the periphery.<sup>21</sup> These authors noted that circulating ANGPTL2 levels paralleled levels of NT-pro BNP and of LAD as measured by UCG, and that those parameters were inversely correlated with %EF, as measured by UCG.<sup>21</sup> In this study, we also observed a positive correlation of circulating ANGPTL2 levels with LAD and an inverse correlation of those levels with %EF in DCM patients. Taken together, circulating ANGPTL2 concentrations increase in subjects with cardiac dysfunction, and may correlate with cardiac dysfunction not only in DCM patients but in patients showing other types of HF, although larger-scale patient studies are required for confirmation. Moreover, additional investigations are needed to determine whether circulating ANGPTL2 concentrations decrease as cardiac dysfunction improves.

A recent study by our group demonstrates that pathological stimuli, such as hypertension, activate ANGPTL2 production in cardiomyocytes, and that heart-derived ANGPTL2 directly contributes to increased circulating ANGPTL2 in HF conditions.<sup>20</sup> Interestingly, the present study revealed that cardiomyocytes are a major source of circulating ANGPTL2 protein in mice after TAC surgery. However, suppression of cardiomyocyte-derived ANGPTL2 in mice did not lower circulating ANGPTL2 levels to baseline levels seen before TAC surgery (**Figure 3C**). Relevant to this, it is noteworthy that ANGPTL2 protein production significantly increased in mouse vWAT and BAT, as well as heart tissues after TAC surgery relative to sham-operated controls, suggesting that after TAC, adipose tissue contributes to increased levels of circulating ANGPTL2. More interestingly, ANGPTL2 protein production was significantly decreased in mice lung and liver after TAC surgery relative to sham-operated controls (**Figure 4A**); however, mechanisms underlying this change remain unclear. We conclude that increased levels of circulating ANGPTL2 after TAC are likely secondary phenomena caused by altered ANGPTL2 secretion from various organs as a result of HF, and that increased ANGPTL2 levels are not an adequate biomarker for HF.

ANGPTL2 is an adipocyte-derived inflammatory mediator that promotes chronic adipose tissue inflammation and systemic insulin resistance.<sup>12</sup> Thus, it is noteworthy that ANGPTL2 expression in adipose tissue increases when HF occurs and is promoted by TAC. This outcome might be exacerbated by induction of adipose tissue inflammation and subsequent resistance in HF conditions,<sup>28–30</sup> an idea supported by observations that circulating ANGPTL2 levels increase in subjects with adipose tissue inflammation and/or insulin resistance.<sup>12</sup> Overall, given these findings, it would be useful to determine whether ANGPTL2 mediates adipose tissue inflammation and subsequent systemic insulin resistance in patients with HF. In contrast, insulin resistance and/or diabetes predisposes patients to HF,<sup>31</sup> creating a vicious cycle of HF and anomalous glucose

metabolism that likely accelerates progression of both conditions and is potentially exacerbated by ANGPTL2. This possibility should be addressed in future studies.

Here, we found that circulating ANGPTL2 levels in sham-operated mice injected with AAV6-shANGPTL2 were comparable to that of shRNA controls, as anticipated (**Figure 3B**). We also found that circulating ANGPTL2 levels in sham-operated *Angptl2<sup>Flox/Flox</sup>* mice were comparable to those seen in sham-operated *Angptl2<sup>Flox/Flox</sup>;αMHC-Cre* mice (**Figure 3C**), suggesting that cardiomyocyte-secreted ANGPTL2 has a lower contribution to circulating ANGPTL2 concentrations in mice without HF.

Our recent study demonstrated that ANGPTL2 secreted from cardiomyocytes perturbs LV contractile ability by inactivating AKT-SERCA2a signaling and decreasing myocardial energy metabolism in *αMHC-Angptl2* Tg mice.<sup>20</sup> However, in that paper, it has not been clarified whether ANGPTL2 affects cardiomyocyte in an endocrine or an autocrine/paracrine manner, because ANGPTL2 protein is a secreted glycoprotein.<sup>12</sup> In this study, we clarified that ANGPTL2 affects cardiomyocytes in an autocrine/paracrine manner, but does not show an endocrine effect on cardiomyocytes. This is consistent with our findings of the in vitro cardiomyocyte experiment where effective ANGPTL2 protein concentration levels were more than 5 μg/mL<sup>20</sup> and greatly exceeded circulating ANGPTL2 protein concentration levels (~1.2 ng/mL) in mice with HF. Thus, increased levels of circulating ANGPTL2 seen in mice with HF are a secondary effect of increased ANGPTL2 secretion from stressed hearts in HF pathologies.

In the present study, we show that based on analysis of *K14-Angptl2* Tg mice and genetically obese diabetic mice, circulating ANGPTL2 alone is not sufficient enough to induce a pathological cardiac response. An alternative way to address this question would be to chronically infuse mice with the ANGPTL2 protein to assess a potential endocrine effect on heart function; unfortunately, we were unable to prepare sufficiently high concentrations of recombinant ANGPTL2 protein required to conduct such an analysis. Nonetheless, further investigations of this type may be required to assess potential endocrine effects of ANGPTL2 on cardiac function.

In summary, circulating ANGPTL2 levels increase in HF patients and mouse models of HF. Those increases are primarily due to enhanced ANGPTL2 secretion from cardiomyocytes, although adipose tissue-derived ANGPTL2 also contributes to those increases. However, we observed no endocrine effect of circulating ANGPTL2 on cardiac function, which suggests that increased circulating ANGPTL2 levels in HF patients reflect, rather than promote, cardiac dysfunction.

### Funding Sources

This work was supported by the Scientific Research Fund of the Ministry of Education, Culture, Sports, Science and Technology (MEXT) of Japan (grants 26293190, 16K15445, and 15H01520 to Y.O., grant 16K09504 to K.M., and grant 16K21236 to Z.T.), and by the Core Research for Evolutional Science and Technology (CREST) program of the Japan Science and Technology Agency (JST) (grant 13417915 to Y.O.). The work was also supported by the CREST program of the Japan Agency for Medical Research and Development (AMED) (grant 15gm0610007h0003, 16gm0610007h0004 and 17gm0610007h0005 to Y.O.).

### Disclosures

None.

## Acknowledgments

We thank our colleagues for valuable suggestions and discussion. We also thank K. Tabu, M. Nakata, S. Iwaki, Y. Shougenji, N. Shirai, and M. Kamada for technical assistance.

## References

- Kannel WB. Incidence and epidemiology of heart failure. *Heart Fail Rev* 2000; **5**: 167–173.
- Stewart S, MacIntyre K, Hole DJ, Capewell S, McMurray JJ. More 'malignant' than cancer?: Five-year survival following a first admission for heart failure. *Eur J Heart Fail* 2001; **3**: 315–322.
- Ambrosy AP, Fonarow GC, Butler J, Chioncel O, Greene SJ, Vaduganathan M, et al. The global health and economic burden of hospitalizations for heart failure: Lessons learned from hospitalized heart failure registries. *J Am Coll Cardiol* 2014; **63**: 1123–1133.
- Lloyd-Jones DM, Larson MG, Leip EP, Beiser A, D'Agostino RB, Kannel WB, et al. Lifetime risk for developing congestive heart failure: The Framingham Heart Study. *Circulation* 2002; **106**: 3068–3072.
- Berry JD, Dyer A, Cai X, Garside DB, Ning H, Thomas A, et al. Lifetime risks of cardiovascular disease. *N Engl J Med* 2012; **366**: 321–329.
- Okura Y, Ramadan MM, Ohno Y, Mitsuma W, Tanaka K, Ito M, et al. Impending epidemic: Future projection of heart failure in Japan to the year 2055. *Circ J* 2008; **72**: 489–491.
- Shimokawa H, Miura M, Nochioka K, Sakata Y. Heart failure as a general pandemic in Asia. *Eur J Heart Fail* 2015; **17**: 884–892.
- Santulli G. Angiopoietin-like proteins: A comprehensive look. *Front Endocrinol (Lausanne)* 2014; **5**: 4.
- Kim I, Moon SO, Koh KN, Kim H, Uhm CS, Kwak HJ, et al. Molecular cloning, expression, and characterization of angiopoietin-related protein: Angiopoietin-related protein induces endothelial cell sprouting. *J Biol Chem* 1999; **274**: 26523–26528.
- Kubota Y, Oike Y, Satoh S, Tabata Y, Niikura Y, Morisada T, et al. Cooperative interaction of Angiopoietin-like proteins 1 and 2 in zebrafish vascular development. *Proc Natl Acad Sci U S A* 2005; **102**: 13502–13507.
- Oike Y, Tian Z, Miyata K, Morinaga J, Endo M, Kadomatsu T. ANGPTL2: A new causal player in accelerating heart disease development in the aging. *Circ J* 2017; **81**: 1379–1385.
- Tabata M, Kadomatsu T, Fukuhara S, Miyata K, Ito Y, Endo M, et al. Angiopoietin-like protein 2 promotes chronic adipose tissue inflammation and obesity-related systemic insulin resistance. *Cell Metab* 2009; **10**: 178–188.
- Tazume H, Miyata K, Tian Z, Endo M, Horiguchi H, Takahashi O, et al. Macrophage-derived angiopoietin-like protein 2 accelerates development of abdominal aortic aneurysm. *Arterioscler Thromb Vasc Biol* 2012; **32**: 1400–1409.
- Tian Z, Miyata K, Tazume H, Sakaguchi H, Kadomatsu T, Horio E, et al. Perivascular adipose tissue-secreted angiopoietin-like protein 2 (Angptl2) accelerates neointimal hyperplasia after endovascular injury. *J Mol Cell Cardiol* 2013; **57**: 1–12.
- Horio E, Kadomatsu T, Miyata K, Arai Y, Hosokawa K, Doi Y, et al. Role of endothelial cell-derived angptl2 in vascular inflammation leading to endothelial dysfunction and atherosclerosis progression. *Arterioscler Thromb Vasc Biol* 2014; **34**: 790–800.
- Aoi J, Endo M, Kadomatsu T, Miyata K, Nakano M, Horiguchi H, et al. Angiopoietin-like protein 2 is an important facilitator of inflammatory carcinogenesis and metastasis. *Cancer Res* 2011; **71**: 7502–7512.
- Endo M, Nakano M, Kadomatsu T, Fukuhara S, Kuroda H, Mikami S, et al. Tumor cell-derived angiopoietin-like protein ANGPTL2 is a critical driver of metastasis. *Cancer Res* 2012; **72**: 1784–1794.
- Odagiri H, Kadomatsu T, Endo M, Masuda T, Morioka MS, Fukuhara S, et al. The secreted protein ANGPTL2 promotes metastasis of osteosarcoma cells through integrin  $\alpha 5 \beta 1$ , p38 MAPK, and matrix metalloproteinases. *Sci Signal* 2014; **7**: ra7.
- Kadomatsu T, Endo M, Miyata K, Oike Y. Diverse roles of ANGPTL2 in physiology and pathophysiology. *Trends Endocrinol Metab* 2014; **25**: 245–254.
- Tian Z, Miyata K, Kadomatsu T, Horiguchi H, Fukushima H, Tohyama S, et al. ANGPTL2 activity in cardiac pathologies accelerates heart failure by perturbing cardiac function and energy metabolism. *Nat Commun* 2016; **7**: 13016.
- Huang CL, Wu YW, Wu CC, Hwang JJ, Yang WS. Serum angiopoietin-like protein 2 concentrations are independently associated with heart failure. *PLoS One* 2015; **10**: e0138678.
- Report of the WHO/ISFC task force on the definition and classification of cardiomyopathies. *Br Heart J* 1980; **44**: 672–673.
- Okamoto R, Hirashiki A, Cheng XW, Yamada T, Shimazu S, Shinoda N, et al. Usefulness of serum cardiac troponins T and I to predict cardiac molecular changes and cardiac damage in patients with hypertrophic cardiomyopathy. *Int Heart J* 2013; **54**: 202–206.
- Cheitlin MD, Armstrong WF, Aurigemma GP, Beller GA, Bierman FZ, Davis JL, et al. ACC/AHA/ASE 2003 guideline update for the clinical application of echocardiography: Summary article: A report of the American College of Cardiology/American Heart Association Task Force on Practice Guidelines (ACC/AHA/ASE Committee to Update the 1997 Guidelines for the Clinical Application of Echocardiography). *Circulation* 2003; **108**: 1146–1162.
- Oka T, Maillet M, Watt AJ, Schwartz RJ, Aronow BJ, Duncan SA, et al. Cardiac-specific deletion of Gata4 reveals its requirement for hypertrophy, compensation, and myocyte viability. *Circ Res* 2006; **98**: 837–845.
- Morinaga J, Kadomatsu T, Miyata K, Endo M, Terada K, Tian Z, et al. Angiopoietin-like protein 2 increases renal fibrosis by accelerating transforming growth factor- $\beta$  signaling in chronic kidney disease. *Kidney Int* 2016; **89**: 327–341.
- Sano M, Minamino T, Toko H, Miyauchi H, Orimo M, Qin Y, et al. p53-induced inhibition of Hif-1 causes cardiac dysfunction during pressure overload. *Nature* 2007; **446**: 444–448.
- Ashrafian H, Frenneaux MP, Opie LH. Metabolic mechanisms in heart failure. *Circulation* 2007; **116**: 434–448.
- Witteles RM, Fowler MB. Insulin-resistant cardiomyopathy: clinical evidence, mechanisms, and treatment options. *J Am Coll Cardiol* 2008; **51**: 93–102.
- Shimizu I, Yoshida Y, Katsuno T, Tateno K, Okada S, Moriya J, et al. p53-induced adipose tissue inflammation is critically involved in the development of insulin resistance in heart failure. *Cell Metab* 2012; **15**: 51–64.
- Opie LH. The metabolic vicious cycle in heart failure. *Lancet* 2004; **364**: 1733–1734.

## Supplementary Files

### Supplementary File 1

**Table S1.** Primer sequences used in quantitative RT-PCR

Please find supplementary file(s);

<http://dx.doi.org/10.1253/circj.CJ-17-0327>